D. M. Burland
D. Haarer

One- and Two-Photon Laser Photochemistry in Organic Solids

The criteria for site-selective low-temperature laser photochemistry in organic solids are discussed within a general framework that includes both one- and two-photon photochemical reaction schemes. We identify requirements for the use of this photochemistry in photochemical hole burning applications such as high-resolution spectroscopy and the study of low-temperature reaction mechanisms. The one- and two-photon reaction schemes are quite different from one another with respect to excited state geometries and short-lived photoreactive intermediates. The reversible tautomerism of quinizarin in hydrogen-bonded host materials is studied as a one-photon example. The photochemistry involves both intra- and intermolecular hydrogen bonds. The photodissociations of s-tetrazine (ST) and dimethyl-s-tetrazine (DMST) are studied as examples of the two-photon reaction and a kinetic scheme is proposed for the tetrazine case. The intensity dependence of the photochemistry in solids is modeled mathematically.

Introduction

The development and ready availability of lasers have had profound influence on the field of photochemistry. Their high intensity and extreme monochromaticity have made it possible to study photochemical reactions in previously unimagined detail [1]. Most previous work on laser photochemistry has involved gas or liquid phases. We wish here to discuss the relatively new area of photochemistry in the solid state at low temperatures (<10 K). The low-temperature solid state aspect brings to the photochemical process several unique features such as the possibilities of unusual reaction pathways, of stabilizing reaction intermediates, and of reversing reactions optically. It has recently been suggested that such solid state photochemical systems can be used as the basis for a high-bit-density memory system [2]. It has also been suggested that such photochemistry can be an extremely efficient means of isotope separation [3].

Both of these applications require materials systems with low-temperature absorption spectra consisting of strong zero-phonon lines and relatively weak phonon sidebands. We discuss criteria for the appearance of strong zero-phonon lines and illustrate these criteria by specific discussions of two photochemical systems, quinizarin and tetrazine. Our emphasis is on the use of these materials in photochemical hole burning applications.

Photochemical hole burning—general remarks

Conventional low-temperature spectroscopy of defects or impurity centers in solids is limited in its spectral resolution by the phenomenon of inhomogeneous broadening. This situation is symbolically depicted in Fig. 1(a), which shows the optical linewidth of a matrix-isolated absorber (*e.g.*, an organic defect center) at low temperatures. At these temperatures each single atomic or molecular defect center has an "intrinsic" linewidth $\Delta\omega_h$ (where h stands for homogeneous) that is given by a radiative or radiationless optical lifetime T_1 and by a dephasing time T_2'. The dephasing time defines the time interval during which the coherence of the excited state is destroyed by phonons. The total homogeneous linewidth is given by [4]

$$\Delta\omega_h = \frac{1}{2T_1} + \frac{1}{T_2'} = \frac{1}{T_2} . \quad (1)$$

At sufficiently low temperatures, where phonon scattering processes can be neglected, the homogeneous line-

Copyright 1979 by International Business Machines Corporation. Copying is permitted without payment of royalty provided that (1) each reproduction is done without alteration and (2) the *Journal* reference and IBM copyright notice are included on the first page. The title and abstract may be used without further permission in computer-based and other information-service systems. Permission to *republish* other excerpts should be obtained from the Editor.

width is, in many instances, determined by the excited state lifetime T_1 [5, 6].

The inhomogeneous linewidth $\Delta\omega_i$, which is generally the low-temperature linewidth in a straightforward absorption experiment, is associated with the envelope of a Gaussian intensity distribution of homogeneously broadened transitions as depicted in Fig. 1(a). The Gaussian distribution is a consequence of the statistical distribution of resonance frequencies of the optical centers due to a variation in local environment in glassy and amorphous matrices and to some extent in crystalline matrices [7, 8].

There are various experimental methods to determine the homogeneous linewidth $\Delta\omega_h$ when it is spectroscopically masked by the inhomogeneous broadening mechanism. We discuss only one of these methods, namely photochemical hole burning (PHB) and the related low-temperature photochemistry. Other methods for resolving $\Delta\omega_h$ are discussed elsewhere [6]. Photochemical hole burning is closely related to selective saturation experiments first performed at radio frequencies in the nuclear magnetic resonance experiments of Bloembergen, Purcell, and Pound [9]. In selective saturation experiments a narrow ($\Delta\omega << \Delta\omega_h$) electromagnetic source, which can have optical or rf frequency, saturates a transition in a two-level system such that only molecules or centers which are in resonance with the light source are affected. If the irradiation is of sufficient intensity to saturate the transition, a *hole* of width $\Delta\omega_h$ is "burned" into the inhomogeneous absorption profile, as shown in Fig. 1(b). The lifetime of the hole corresponds to the excited state lifetime; its width corresponds, at sufficiently low irradiation intensities where saturation broadening effects [10] can be neglected, to the homogeneous linewidth $\Delta\omega_h$. This width is an intrinsic parameter of the absorbing impurity center or defect at a given temperature. The first optical saturation experiment in the solid state was performed in ruby by Szabo [11].

Photochemical hole burning experiments are a variation of the saturation experiments just described, with two main differences. First, the impurity center is photochemically unstable upon irradiation into the inhomogeneously broadened transition. Therefore, the created hole is relatively stable at low temperatures; in this sense PHB is not a transient phenomenon. Second, the narrow irradiation does not have to saturate the optical transition. It merely has to provide enough photons, integrated over the irradiation time, to photochemically convert a measurable fraction of the absorbers.

The first relevant papers on PHB phenomena were published in 1974 by two Russian groups [12, 13]. The high-

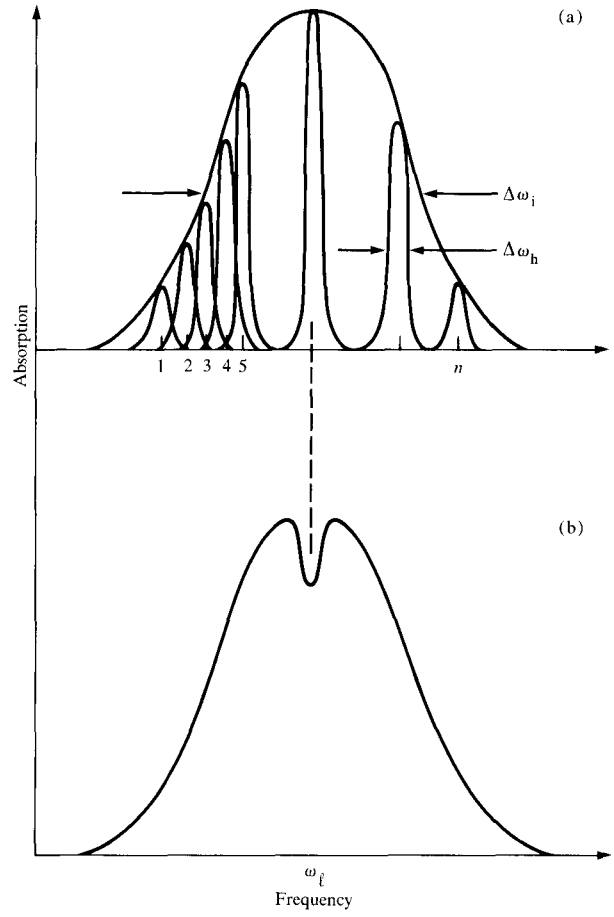

Figure 1 (a) Symbolic representation of an inhomogeneous absorption line as a superposition of n distinguishable sites of the width $\Delta\omega_h$. (b) Line profile during optical saturation or after photochemical reaction with light of frequency ω_ℓ, showing burned hole.

resolution potential was first demonstrated by Gorokhovskii *et al.* [14] and by de Vries and Wiersma [15]. At the time of the first PHB experiments the hole burning phenomena were primarily investigated from the viewpoint of providing a new technique in high-resolution optical spectroscopy. In the following section we discuss some aspects of the specific photochemistry required for photochemical hole burning. Some of the requirements are quite restrictive, ruling out many of the well-known photochemical systems. In particular, most photochromic systems cannot be used in PHB applications.

Zero-phonon requirements in one- and two-photon photochemical schemes

The scheme of photochemistry symbolically depicted in Fig. 1(b) may be described as site-selective. The word *site* can be used here in a dual sense. In a crystalline environ-

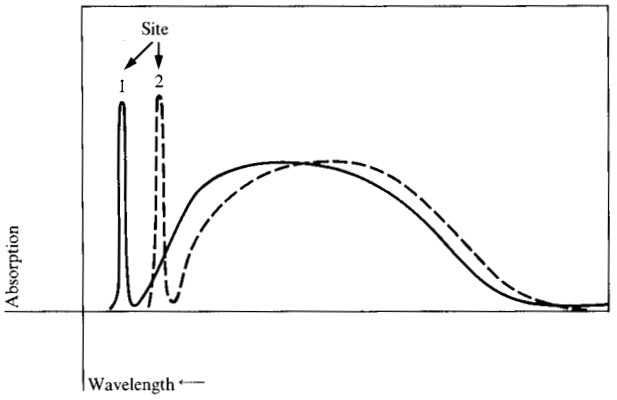

Figure 2 Symbolic spectrum of two different sites in a solid. Each site has a sharp zero-phonon transition and a broad continuum-like phonon sideband.

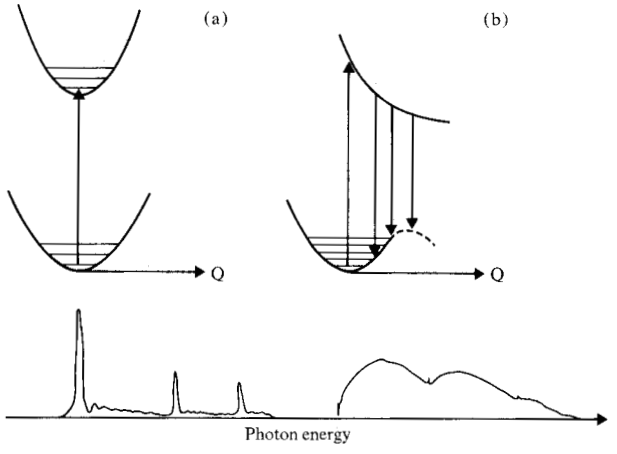

Figure 3 Configuration coordinate schemes and absorption spectra (lower curves) for weak (a) and strong (b) electron-phonon coupling (see text).

ment a certain well-defined geometric host-guest configuration can be called a site. The number of sites in this sense depends on the size and symmetry of the guest molecule with respect to the host environment. The word site can also be used to describe a local host-guest configuration in a random or crystalline environment containing strain fields and other inhomogeneities without specific further changes of the local geometry. In both definitions, the term site-selective photochemistry implies that only a subset of the total number of molecules is involved, namely the subset that is in resonance with the laser light.

Site-selective photochemistry as just defined can only be achieved in a purely electronic or vibrational transition that is characterized by a well-defined transition frequency. When optical bands are broadened by a phonon continuum, as for instance in the case of phonon-induced spectral sidebands, the site-selective PHB phenomenon disappears due to the continuum nature of the transitions. This situation is depicted in Fig. 2, which is a schematic illustration of the absorption spectra of two different sites. Each spectrum consists of a zero-phonon transition and its corresponding phonon sideband. From the figure one can see that selective excitation can be achieved only in the electronic origin of site 1 or site 2.

Having this *zero-phonon criterion* in mind, one can categorize optical spectra into two general classes. Class one, symbolized in Fig. 3(a), represents the case of a "rigid" excited state with little or no rearrangement in bonds or the lattice after the optical excitation. The configuration coordinate picture is given at the top of the figure; Q represents either a molecular coordinate for vibrons or a lattice coordinate for phonons. Figure 3(a) shows that with no bond rearrangement the optical transition is, at low temperatures, purely electronic in its character if one assumes linear electron-phonon coupling. The arrow in the Franck-Condon scheme originates at the level of zero-point vibrations where no thermal modes are excited. The corresponding optical spectrum is therefore mostly of zero-phonon character, with a weak phonon sideband and a progression of intramolecular vibron modes. Each of the zero-phonon peaks, however, corresponds to an inhomogeneously broadened band such as that shown in Fig. 1.

As soon as the excited state is "displacive," as in many transitions leading to photochemical dissociations, the configuration coordinate scheme looks like Fig. 3(b). Here the upper state is dissociative and the optical transitions are characterized by a considerable admixture of phonon levels. This admixture of continuum states smears out the well-defined electronic and vibronic transitions and leads to a spectrum like that shown in Fig. 3(b). In this case the line broadening is dynamic and very similar to the one observed for organic charge-transfer states with displacive excited states ([16] and references therein) and for molecules that dissociate in their excited state [17]. This dynamical broadening cannot be eliminated with laser spectroscopy and thus represents a major limitation in the application of PHB spectroscopy to many photochemical systems.

With these limitations in mind, one can divide PHB photochemistry into two classes. The first class involves single-photon photochemistry in which the excited state lives long enough to give rise to a sharp optical transition. A typical example would be a system with an activation barrier or a level crossing in the excited state, as shown in Fig. 4(a). The second class involves two-photon pho-

tochemistry [Fig. 4(b)] in which the initial photon achieves the site selection and the second photon is responsible for the subsequent photochemical reaction. It should be noted that in both of the strategies outlined in Fig. 4 for avoiding broad phonon sidebands, the initially excited state is not dissociative. Rather, the system evolves from this state into a dissociative state either in a radiationless process [Fig. 4(a)] or by absorption of an additional photon [Fig. 4(b)]. All PHB systems whose mechanisms are known at the present time fit into one of these two classes. We now discuss an example of each of the two mechanisms.

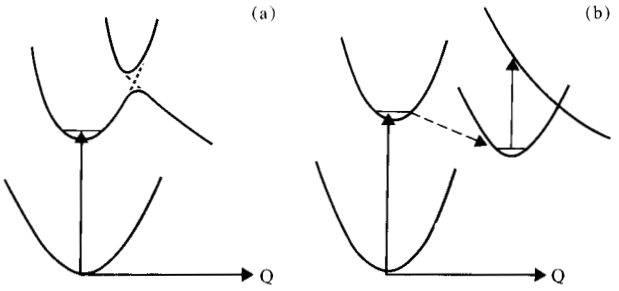

Figure 4 Schemes for one-photon (a) and two-photon (b) photochemistry that preserve the zero-phonon nature of the optical transition.

One-photon photochemistry

• *The photochemistry of quinizarin*

As we have pointed out in the previous section, one-photon photochemistry is the most straightforward scheme for PHB. Yet it seems difficult within this scheme to fulfill the Franck-Condon requirements for zero-phonon transitions and, at the same time, to have a reasonable chemical reaction probability. The known photoreactive systems based on one-photon processes are either of a "photophysical" nature (*i.e.*, a rigid absorber reorienting geometrically in the excited state and thus changing its position within the inhomogeneous line profile [12, 18]), or sytems belonging to a class that can be categorized as exhibiting "slow" photochemical reactions involving the long-lived triplet levels of the system [19].

We now consider a different mechanism involving a reversible one-photon reaction that occurs on the time scale of tens of picoseconds and associated with a rearrangement of hydrogen bonds. Preliminary evidence for this phenomenon has been reported very recently [20]. The type of intramolecular proton transfer process of interest in this section can be depicted as follows:

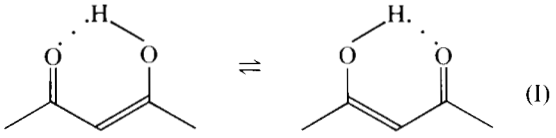

(I)

The photoreactive group in Scheme (I) is the six-member ring in which the hydrogen atom participates in a covalent bond with one of the oxygens and a hydrogen bond with the carbonyl oxygen. As one can see from this scheme, the transfer of a proton in the excited state leads to tautomers [Structures (B) in Fig. 5] in which the covalent bond and the hydrogen bond are interchanged.

Figure 5 shows the molecule quinizarin [Structure (A)] (1,4-dihydroxyanthraquinone), which can be considered as a model system for a molecule exhibiting intramolecular hydrogen bonds and also having the basic requirements for light-induced tautomerism [Structures (B)]. The tautomeric transformation can involve one or both of the protons shown in the figure. This process requires only a rearrangement of molecular conjugation and results in a net C—O bond length change on the order of 0.1 Å (0.01 nm). This is to be expected as a consequence of the difference between carbon and oxygen single and double bonds [21] and is confirmed from the crystal structure of a related compound (1,5-dihydroxyanthraquinone) in which the protons are believed to be localized. The C—O double bond is about 0.01 nm shorter (0.121 nm) than the corresponding C—O single bond (0.134 nm); see Ref. [22].

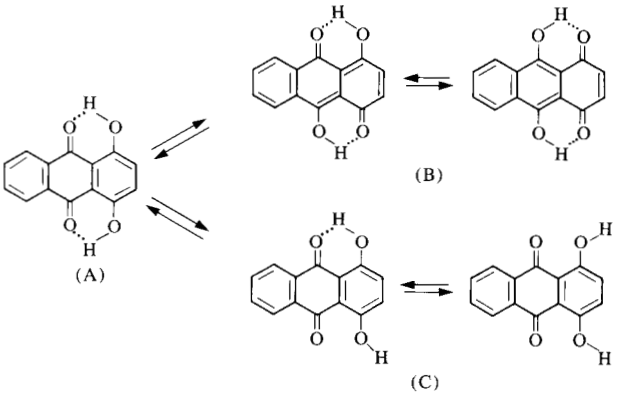

Figure 5 Structures of quinizarin (A) and the possible tautomers (B) and conformers (C) that allow the formation of hydrogen bonds with the matrix.

Also depicted in Fig. 5 is the mildest version of a possible photochemical reaction. It shows two possible conformers [Structures (C)] of the molecule in which, in contrast to the tautomeric structures, all double and single bonds of the molecule remain unchanged and only a pe-

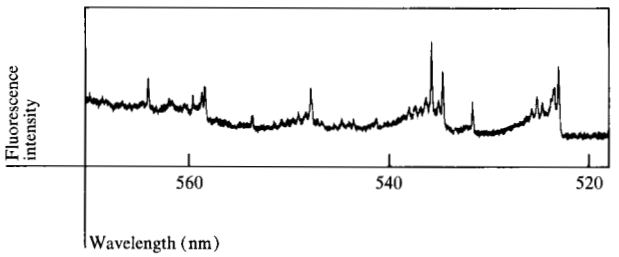

Figure 6 Fluorescence emission spectrum of quinizarin in n-heptane at 2 K.

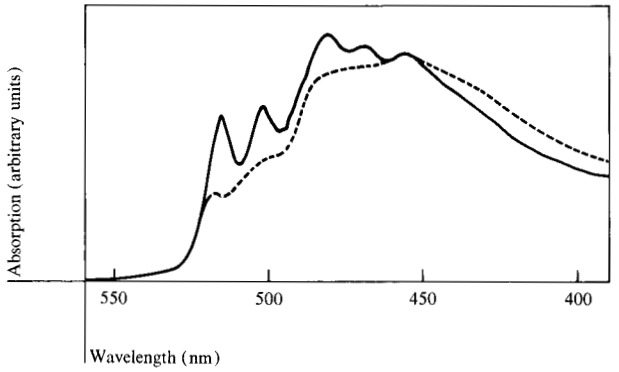

Figure 7 Low-resolution absorption spectrum of quinizarin in an ethanol/methanol glass at 2 K (solid line) and the same spectrum after broad band photochemistry (dashed line).

ripheral bond angle is being changed. In the specific case shown, two *rotamers* are formed by rotating the proton around the C—O axis. We subsequently present evidence that the observed hole burning phenomenon is, in fact, due to the formation of such rotamers, which allow hydrogen bonding between the transformed molecule and the matrix. We also present quantitative data on electron-phonon coupling and draw some preliminary conclusions on the dynamics of the proton transfer process.

• *Experiments in non-hydrogen-bonded matrices*

If one dopes quinizarin at a molar concentration of about 10^{-5} into n-alkane matrices like heptane, which are known to yield zero-phonon-type molecular spectra [23], one obtains a very structured fluorescence emission spectrum, as shown in Fig. 6. The spectrum was taken at 2 K using the 435.8-nm line of a 100-W Hg lamp as the excitation source; the doped sample was polycrystalline. The structured spectrum shows a characteristic zero-phonon origin at 522.6 nm and its vibrational satellites. The optical lines show the usual inhomogeneous broadening, which in this case is on the order of 10 cm^{-1}. Since the lowest singlet transition of quinizarin has its main oscillator strength in the electronic origin and in its vibronic satellites, one can conclude that it fulfills the zero-phonon conditions required for site-selective photochemistry.

In a systematic study, quinizarin was investigated in different non-hydrogen-bonded matrices such as the n-alkanes, single-crystalline phenanthrene, and methyltetrahydrofuran glass [20, 24]. We irradiated into the 0-0 transition (522.6 nm in heptane) with a narrow band dye laser ($\Delta\omega_\ell$ corresponding to <0.01 nm spectral bandwidth) and looked for photochemical changes via excitation spectroscopy as described in [5]. Under the conditions of our experiment we could not find measurable photoinduced spectral changes and thus concluded that the optical quantum yield of the photochemical reaction must be smaller than 10^{-4}. Our findings appear to confirm earlier experimental data in related systems [25].

From our experiments we conclude that there is no measurable intramolecular proton transfer of the type illustrated in Fig. 5 [Structures (B)] under our experimental conditions in aprotic matrices. This is corroborated by the narrow and well-resolved structure of the optical spectrum (Fig. 6). The normal appearance of the Franck-Condon envelope of the vibrational pattern (an intense 0-0 transition and much weaker vibronic lines) and the very small phonon tails of the transitions do not reflect major changes in the bonds or the geometry of the molecule in the excited state. From previous experiments on dimethylanthraquinone [20], it is known that similar molecules that do undergo low-temperature photochemistry tend to have rather broad and structureless optical spectra.

• *Experiments involving hydrogen-bonded matrices*

Photochemical observations If one dopes quinizarin in molar concentrations of about 10^{-5} into organic glasses that form strong hydrogen bonds, such as a mixture of ethanol (70%) and methanol (30%), the situation changes dramatically. First, the low-temperature spectrum is broadened considerably, reflecting the amorphous nature of the glass. The solid line in Fig. 7 shows a typical absorption spectrum of quinizarin in an alcohol glass at 2 K. The optical bandwidth is on the order of 400 to 500 cm^{-1}, yet the spectrum reflects the same vibrational features visible in the well-resolved fluorescence spectrum in heptane (Fig. 6). Second, the molecule, which was photochemically inactive in other environments, exhibits photochemical changes that occur with comparatively high yield. Figure 7 (dashed line) shows the same spectrum in a low-resolution scan after the sample had been irradiated for ten minutes each at wavelengths of 513, 515, and

517 nm with diffuse laser light of several mW/cm^2 power. From Fig. 7 one sees that the structured part of the spectrum disappears to yield a photoproduct showing a broad band absorption at wavelengths shorter than 450 nm; the energy separation between the initially absorbing species and the photoproduct is slightly larger than 2000 cm^{-1}. The observed photochemistry is thermally reversible; *i.e.*, the original spectrum reappears after the sample is warmed to 80 K [25].

The reversibility of the reaction, the magnitude of the spectral shift, and the matrix dependence of the experiment rule out irreversible photochemical transformation of the quinizarin molecule. The fact that the photochemistry occurs only in hydrogen-bonded matrices strongly suggests a reaction involving both the intra- and intermolecular hydrogen bonds. In a very simple molecular orbital calculation [20] we have shown that the formation of a hydrogen-bonded conformer, in which the intramolecular hydrogen bond is broken and an intermolecular hydrogen bond is formed, as depicted in Fig. 5, could be expected to raise the energy of the ground state by about 1400 cm^{-1}. It is commonly assumed that hydrogen bonds affect a localized ground state more than a delocalized excited state [26], so that the ground state calculation can be taken as a reasonable estimate for the expected photochromic shift. Within this approximation, the measured shift (2000 cm^{-1}) is consistent with the suggested model of conformers (C) in Fig. 5. Other possible mechanisms that involve a complete proton transfer from the quinizarin molecule to the matrix can be ruled out on the basis of absorption experiments with samples of deprotonated quinizarin [24]. Within the above model we cannot decide at this time whether one or both of the quinizarin protons are involved in the transformation. The answer to this question requires more accurate calculations and experiments with differently substituted molecules.

Electron-phonon coupling From the broad band spectrum of Fig. 7 we cannot determine whether the zero-phonon nature of the lowest singlet transition of quinizarin is preserved in the amorphous hydrogen-bonded matrices. We have seen earlier that the strength of the electron-phonon coupling is an important parameter in our effort to use PHB as a tool for high-resolution spectroscopy. It is also important in the assessment of possible usage of PHB phenomena in ultrahigh-density storage schemes [2]. Figure 8 shows high-resolution absorption spectra of photochemical holes in two different quinizarin-doped matrices [25]. The spectrum obtained in a film of polyvinyl alcohol is shown in Fig. 8(a) and that obtained in an alcohol glass in Fig. 8(b); both spectra were taken at 2 K. The photochemical holes were created with an argon ion laser at a wavelength of 514.5 nm. Both spectra show a

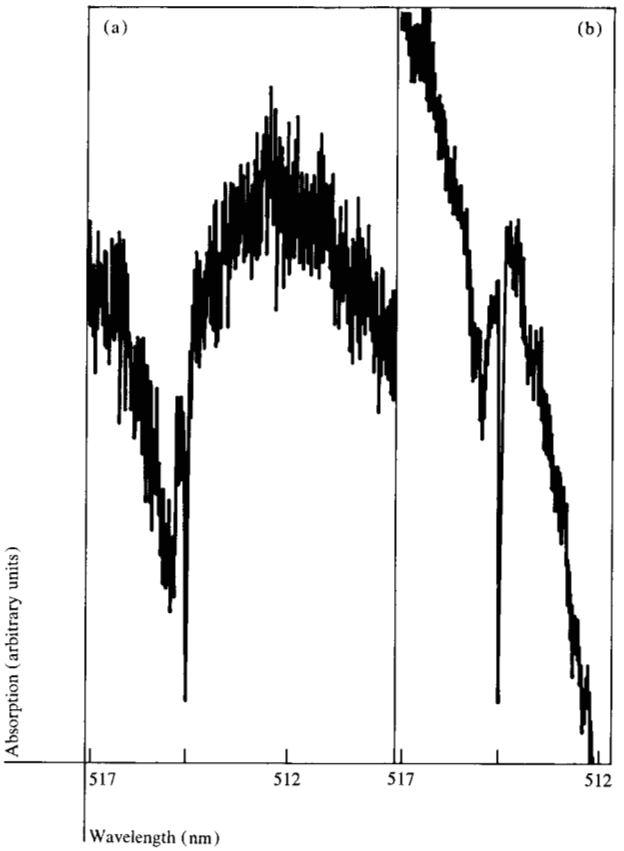

Figure 8 Zero-phonon holes (sharp negative peaks) and phonon "sideholes" in (a) PVA at 2 K and (b) an ethanol/methanol glass at 2 K.

distinct and narrow zero-phonon hole and a pronounced "phonon sidehole" of different intensity. The fact that both phonon sidebands are at the long-wavelength side and not, as is usual for absorption spectra, at the short-wavelength side of the 0-0 transition has been discussed in [18] and is due to the loss of phonon energy during the photochemical cycle.

To discuss the phonon coupling strength, which is obviously different for both matrices, we use a simplified configuration coordinate model which assumes that only one *normal mode* of the lattice couples to the optical transition. This model has been quite successfully used in the description of color center defects [27]. With this model we can determine both the coupling strength and frequency of the active mode. The phonon coupling strength is characterized by the Huang-Rhys factor S. This factor characterizes, in a simplified way, how many quanta of the strongest coupling photon mode are simultaneously excited with the electronic transition. At very low temperatures (compared with the Debye temperature) S fol-

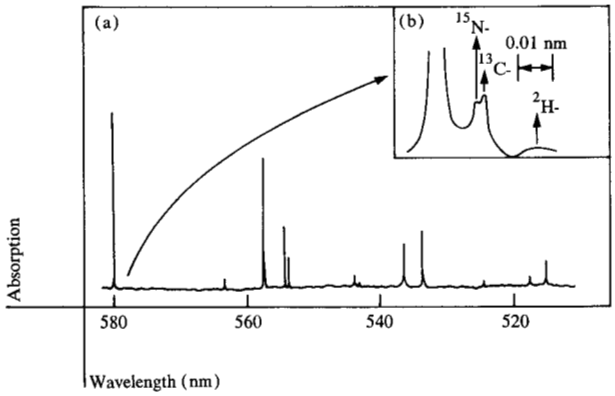

Figure 9 The absorption spectrum of s-tetrazine in benzene at 2 K. (a) Low-resolution scan of S_1 and (b) isotopic fine structure of the absorption origin near 580 nm.

Table 1 Parameters of the normal mode evaluation.

Matrix	S	ω_n (cm^{-1})	$\Delta\omega_z$ (cm^{-1})
PVA	1.84	13.5	2.3 ± 0.8
Ethanol/ methanol	0.99	15.9	1.2 ± 0.4

lows directly from the ratio of the zero-phonon line to the phonon sideband. One can approximate [16, 27, 28] that

$$\frac{I_z}{I_t} \approx \exp(-S), \tag{2}$$

where I_z is the integrated zero-phonon line intensity and I_t is the intensity of the entire band.

The coupling frequency ω_n follows from the same model by evaluating the spectral splitting δ between the zero-phonon origin and the maximum of the phonon sideband according to the relation [16, 27, 28]

$$\delta = S\hbar\omega_n. \tag{3}$$

Table 1 shows the various parameters given by our normal mode evaluation. As is obvious from Fig. 8, the phonon coupling is stronger in polyvinyl alcohol (PVA) than it is in alcohol glasses. The latter can still be considered as weakly coupled ($S < 1$), whereas the PVA matrix exhibits intermediate electron-phonon coupling strengths ($1 < S < 5$). It is interesting to note that both coupling modes have quite low frequencies and their numerical values are very similar. In fact, it is questionable, within the accuracy of the measurements, whether the difference in mode frequency between 13.5 and 15.5 cm^{-1} is significant. The observed trend, however, that matrices with stiffer coupling modes (larger spring constants) show weaker electron-phonon coupling is reasonable and may be relevant. Similar phenomena have been observed in other organic matrices [16]. The trend would indicate that PHB spectroscopy yields higher resolution in matrices that do not have low-lying lattice modes. To confirm this, more experimental information is necessary.

The width of the zero-phonon transition $\Delta\omega_z$ (see Table 1) varied slightly from sample to sample and from one matrix to the other. The comparatively large value of 1–2 cm^{-1} seems to indicate that rapid proton transfer processes occurring on a 10- to 100-ps timescale might be the limiting factor in determining the photochemical hole widths in these systems. This would open the interesting possibility of studying, for the first time, the dynamics of proton transfer processes at very low temperatures. Related aspects of rapid proton transfer have been investigated in the time domain and have been proposed as the first step in the photochemistry of the vision process involving the rhodospin molecule [29].

Two-photon photochemistry

• *The photochemistry of s-tetrazine (ST)*

In this section we discuss a photochemical process that proceeds via the two-photon mechanism shown in Fig. 4(b). We discuss photochemistry that occurs with the sequential absorption of two photons [30] and we exclude consideration of photochemical processes that occur upon the simultaneous absorption of two laser photons without the intervention of a real intermediate energy level [31].

The specific photochemical reaction treated is the photodissociation of s-tetrazine; see Scheme (II):

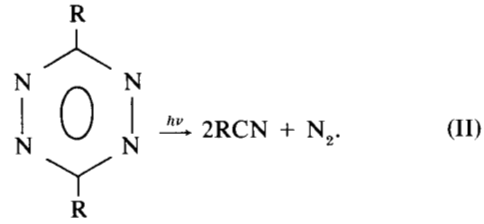

(II)

A variety of tetrazine derivatives have been synthesized and their low-temperature photodissociation studied [32]. We focus in this section on the unsubstituted (R = H) s-tetrazine (ST) and its dimethyl (R = CH_3) derivative (DMST). De Vries and Wiersma have demonstrated photochemical hole burning in both DMST [15] and ST [33]. Interest in these species has been stimulated by the demonstration by Karl and Innes [34] and by Hochstrasser and coworkers [3] that the photodissociation process can be used as a means of efficient separation of nitrogen, carbon, and hydrogen isotopes.

Both PHB and laser isotope separation rely on the fact that the absorption lines of ST and DMST in certain molecular crystal hosts are reasonably sharp and broadened inhomogeneously. Figure 9 shows the absorption spectrum of ST in benzene at 2 K, both the low-resolution scan of S_1 [35] and the detailed isotopic fine structure of the absorption origin near 580 nm [32]. As we have seen, the simultaneous occurrence of sharp inhomogeneously broadened spectral lines and the single-step photodissociation seems to be contradictory. In fact, as we will see, ST and DMST do not photodissociate quite so simply. Until quite recently, Scheme (II) appeared to describe tetrazine photodissociation; however, recent work [36] has shown that the process at low temperature is more complex and more accurately represented by Scheme (III):

$$\xrightarrow{h\nu} S_1 \rightarrow (X_1, \cdots, X_n) \xrightarrow{h\nu'} 2RCN + N_2. \qquad \text{(III)}$$

Here the photodissociation proceeds via the excited singlet state S_1 and through several intermediates (X_1, $\cdots$, X_n) and requires the sequential absorption of two photons. Scheme (II) corresponds to the energy level arrangement shown in Fig. 4(a); Scheme (III), roughly to that shown in Fig. 4(b).

We next describe details of the two-photon tetrazine photodissociation as revealed by laser spectroscopic studies and some theoretical aspects of two-photon photochemistry with particular emphasis on the problems encountered when studying these processes in solids at low temperatures.

• *Two-photon photodissociation*

The first indication that Scheme (I) was an oversimplified description of the tetrazine photodissociation process came from an examination of the relative rates of room temperature photodissociation of ST and DMST in hexane. It was shown by Burland *et al.* [36] that while ST photodissociated with a quantum yield near unity, the DMST photodissociation was at least an order of magnitude less efficient. Furthermore, it was shown that the photodissociation of ST in solution at 300 K, using either a laser or a lamp, was linear in exciting light intensity, consistent with Scheme (II).

These results raised the question as to what was happening with DMST. From the hole burning results of de Vries and Wiersma [15, 33] and the detailed photophysical studies of Hochstrasser *et al.* [32], it was known that DMST photodissociated in mixed molecular crystals, at least at low temperatures. To resolve this problem, Burland *et al.* [36] investigated the intensity dependence of the photodissociation. Using a N_2-pumped pulsed dye laser for excitation and monitoring the extent of photodis-

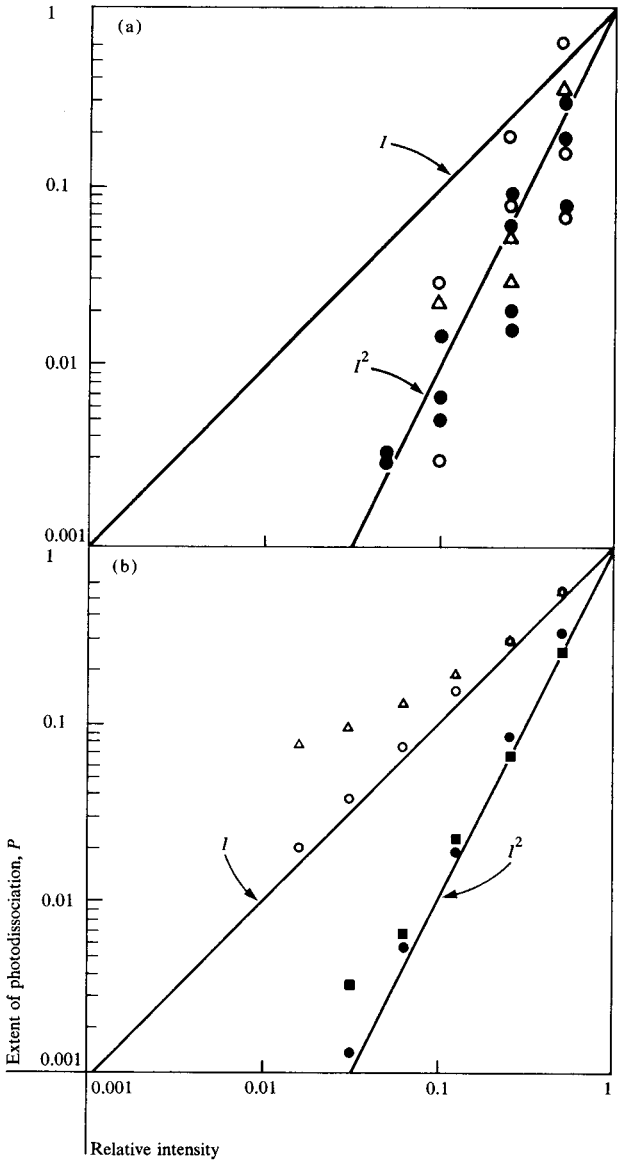

Figure 10 (a) The extent of photodissociation P at 2 K as a function of the exciting light intensity, where P is normalized to unity for the maximum light intensity used in each pulsed dye laser experiment. The data points are for DMST in durene, excitation into the lowest singlet at 587 nm (○); DMST in p-xylene, excitation into the lowest singlet at 588 nm (△); and ST in benzene, excitation into the lowest singlet at 580 nm (●). (b) Calculated P *versus* intensity curves for one-photon (○, △) and two-photon (●, ■) photochemistry at concentrations of 2×10^{-4} (△), 2×10^{-7} (○, ●), and 2×10^{-5} (■) mole-cm^{-3}.

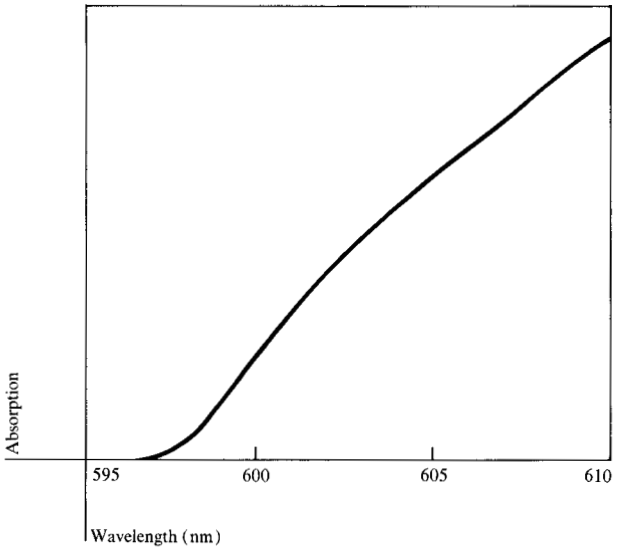

Figure 11 The transient absorption observed in a crystal of DMST in durene at 2 K excited at 587 nm with a 6-ns pulse.

sociation P by following the disappearance of the tetrazine absorption spectrum, they obtained the results shown in Fig. 10(a). The measured quantity P is defined by

$$P = \frac{a_0 - a}{a_0 t}, \tag{4}$$

where the absorption a is given by $-\ln T$ and a_0 is a at time $t = 0$; T is the fraction of light transmitted through the sample. Upon $S_1 \leftarrow S_0$ excitation, the photodissociation of both ST and DMST at low temperature (2 K) had a quadratic dependence on light intensity; this is consistent with Scheme (III). Dellinger *et al.* [37] have recently shown that the photodissociation of DMST in ethanol at room temperature is also quadratic. It has been shown that direct excitation at $h\nu$, where $h\nu$ is the $S_1 \leftarrow S_0$ excitation energy, also results in quadratic photochemistry [36].

These experimental results are consistent with Scheme (III). Excitation into the singlet manifold of tetrazine either directly or indirectly (via radiationless decay of higher states) produces S_1, which then decays through an unknown number of intermediate steps (*vide infra*) to produce the intermediate X_n. Hochstrasser and King [32] have shown that X_n is not the vibrationally relaxed lowest triplet state T_1 by showing that direct excitation of S_1 does not result in triplet population. In the absence of a second photon, X_n simply decays back to the tetrazine ground state S_0. The process $S_0 \rightarrow S_1 \rightarrow X_n \rightarrow S_0$ inhibits the production of T_1. If a second photon is available, X_n dissociates into products. In this mechanism it is necessary that the energy of the second photon overlap at least a part of the X_n absorption spectrum.

The room temperature solution photodissociation of ST does not follow Scheme (III) because its decomposition is linear in light intensity. This can be explained by assuming that one of the ST intermediates is thermally unstable at room temperature and does not require an additional photon for decomposition.

If Scheme (III) correctly describes absorption in the tetrazines, one might observe transient absorption due to the intermediate X_n. In fact, transient absorption has been observed by Dellinger *et al.* [37] and by Burland and Carmona [38]. This absorption, a portion of which is shown in Fig. 11, extends from the origin of the tetrazine $S_1 \leftarrow S_0$ transition down to at least 700 nm, with a maximum at 630 nm [37]. In Fig. 11 the DMST $S_1 \leftarrow S_0$ origin at 587 nm is on the short-wavelength edge of the transient absorption. (The absorption is recorded in a time window that begins 100 ns after the pulse and is 10 ms wide. The figure shows the difference between transmitted light with and without laser excitation.) Thus, according to Scheme (III), when $h\nu_1 = h\nu_2$ the second photon is very inefficiently absorbed by X_n.

Dellinger *et al.* [37] have observed the rise and decay times of X_n using flash photolysis techniques. In degassed ethanolic solutions of DMST at room temperature they observed a rise time of 6 μs and a decay time of 500 μs for the transient absorption. This is to be compared to a singlet state lifetime of 6 ns [32]. The slow rise time of the intermediate absorption indicates that there must be more than one intermediate in this process.

• *Theoretical aspects of two-photon photochemistry*

We now consider two questions arising from the work just discussed on the two-photon tetrazine photodissociation. The first question arises whenever one considers photochemistry in a solid environment; it involves the fact that in a rigid medium the photochemical process and the exponential dependence of light intensity on distance into the sample result in a spatially heterogeneous concentration of reactants, even if one begins with a homogeneous sample. The question we wish to consider is to what extent this heterogeneity can mask our ability to distinguish one- and two-photon photodissociations. Second, we consider the detailed kinetics of the photochemical process expressed by Scheme (III). From this treatment we will be able to explain the initially puzzling result obtained by Dellinger *et al.* [37]. They found that ST in a low-temperature matrix decomposes quadratically under laser illumination and linearly under broad band lamp illumination.

First we treat the solid state absorption problem, by considering the simplified three-level kinetic scheme outlined in Fig. 12(a). For this scheme, the rate equations can be written

$$\frac{d[A^{**}]}{dt} = k_2 I[A^*],$$

$$\frac{d[A^*]}{dt} = k_1 I[A] - \frac{1}{\tau}[A^*] - k_2 I[A^*],$$

$$\frac{d[A]}{dt} = \frac{1}{\tau}[A^*] - k_1 I[A],$$

where the $k_i I$ are rate constants and τ is a lifetime. For optically thin samples, the number of einsteins actually absorbed by the solid sample, I^1_{abs} and I^2_{abs}, can be approximated by

$$I^1_{abs} = k_1 I[A], \qquad I^2_{abs} = k_2 I[A], \tag{5}$$

where k_1 and k_2 depend on the sample thickness and the molar extinction coefficient ϵ of the transitions; [A] represents the concentration of ground state molecules and I the light intensity at a given point in the crystal. Assuming, as is usually done [30], a steady state concentration of the excited state [A*], the rate of disappearance of ground state molecules is given by

$$\frac{d[A]}{dt} = \frac{-k_1 k_2 I^2 \tau}{1 + k_2 I \tau}[A] \approx -k_1 k_2 I^2 \tau [A], \tag{6}$$

where the approximation is valid for light intensities such that $k_2 I\tau << 1$. We also assume the differential form of the Beer-Lambert law:

$$\frac{dI}{dx} = -\alpha[A]t. \tag{7}$$

If we generalize Eq. (6) to

$$\frac{d[A]}{dt} = -\beta[A]I^n, \tag{8}$$

the derived equations are also valid for linear ($n = 1$) processes. The quantities α and β are defined by Eqs. (7) and (8). The equations governing linear photodissociation processes have previously been derived by Simmons [39] and by Mauser [40].

By extending the results of Simmons [39] to nonlinear processes, we obtain for the concentration $[A]_x$ at a point x in the crystal, the following result:

$$[A]_x = \frac{f'(0)}{n\alpha} \times \left(\frac{\exp(-\beta I_0^n t)}{\exp(-\beta I_0^n t)\{1 - \exp[-f(0)]\} + \exp[-f(0)]} \right), \tag{9}$$

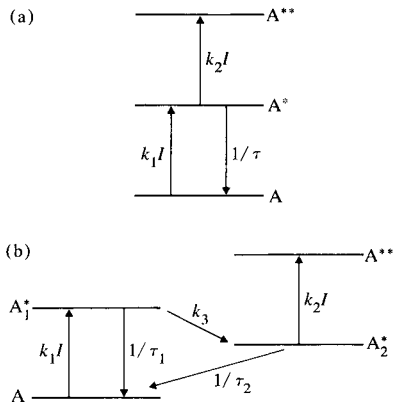

Figure 12 Two kinetic schemes for sequential two-photon absorption: (a) simplified three-level system and (b) four-level system.

where I_0 is the incident light intensity (*i.e.*, the intensity at $x = 0$), $f'(0)$ is the spatial derivative of $f(0)$, and

$$f(0) = n\alpha \int_0^x [A]_x^0 dx. \tag{10}$$

The term $f(0)$ is equal to $n\alpha[A]_x$ when the initial concentration at time $t = 0$ is independent of x.

The fraction of light transmitted through the crystal, $T = I/I_0$, after irradiation for a time t is given by

$$T = \left\{ \frac{1}{1 + \left(\frac{1 - T_0^n}{T_0^n} \right)[\exp(-\beta I_0^n t)]} \right\}^{1/n}, \tag{11}$$

where T_0 is the transmittance at $t = 0$. Using Eq. (11) and assuming that

$$\frac{1}{n}\left(\frac{1 - T_0^n}{T_0^n} \right) << 1, \tag{12}$$

we obtain

$$P \approx \beta I_0^n, \tag{13}$$

where P is defined in Eq. (4). Therefore, in the limit given by Eq. (13), we can use a plot of P *versus* I_0 to determine the quantity n.

To demonstrate in more detail the consequences of Eqs. (9) and (11), we show calculations of $[A]_x$ *versus* x for several initial homogeneous concentrations in Fig. 13. Note that for the lowest initial concentrations, the concentration $[A]_x$ after irradiation is fairly uniform for both linear (one-photon, solid line) and quadratic (two-photon, dashed line) processes. For higher concentrations, the illuminated sample face ($x = 0$) has a much lower concen-

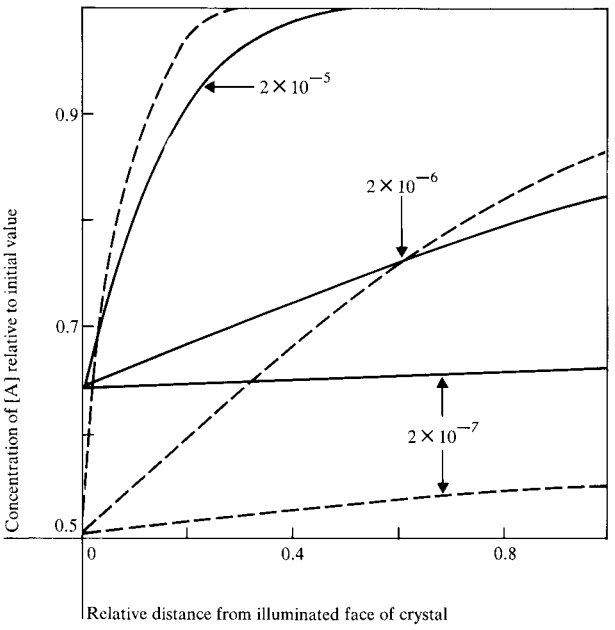

Figure 13 The concentration of A as a function of distance in a crystal undergoing one-photon (solid lines) and two-photon (dashed lines) photochemistry; $\epsilon = 10^3$ liter-mole^{-1}-cm^{-1}, sample thickness of 0.2 cm. The concentration values indicated on the curves are in moles-cm^{-3}; $x = 0$ is the illuminated face and $x = 1.0$ is the unilluminated face.

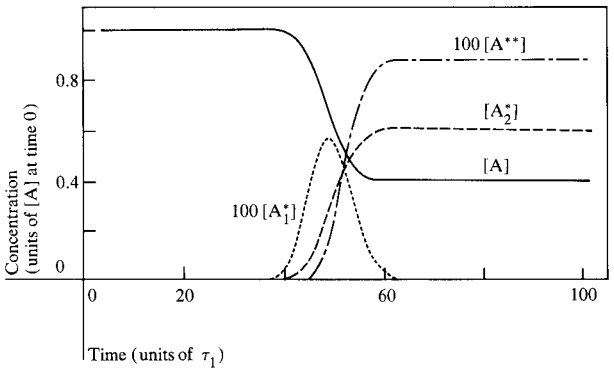

Figure 14 Calculated concentration profiles (see curve labels) of the various intermediates in the four-level reaction scheme shown in Fig. 12(b); 10-μJ pulsed laser, 5-ns pulse width; $\epsilon_1 = 10^5$ liter-mole^{-1}-cm^{-1}, $\epsilon_2 = 10^2$ liter-mole^{-1}-cm^{-1}.

tration after irradiation than does the unilluminated face ($x = 1.0$), as expected. Figure 10(b), a theoretical version of the experimental results shown in Fig. 10(a), shows the calculated quantity P as a function of the laser intensity I_0. For a broad range of concentrations one can determine the order of the process from such P *versus* I_0 plots. Even for the concentration 2×10^{-5} mole/cm^3 (■ data points) in Fig. 10(b), for which Fig. 13 shows a marked concentration inhomogeneity after irradiation, one can clearly distinguish between linear and quadratic processes. From these results it appears that Eq. (12) is an unnecessarily stringent restriction and that Eq. (13) is approximately valid well outside this range.

We next turn to the detailed kinetics of the photochemical process described by Scheme (III); the four-level system is outlined in Fig. 12(b). The kinetic equations are

$$\frac{d[A^{**}]}{dt} = k_2 I[A_2^*],$$

$$\frac{d[A_2^*]}{dt} = k_3[A_1^*] - k_2 I[A_2^*] - \frac{1}{\tau}[A_2^*],$$

$$\frac{d[A_1^*]}{dt} = k_1 I[A] - k_3 I[A_1^*] - \frac{1}{\tau}[A_1^*],$$

$$\frac{d[A]}{dt} = \frac{1}{\tau}[A_1^*] + \frac{1}{\tau}[A_2^*] - k_1 I[A].$$

We have not attempted to obtain an analytical solution to the simultaneous equations but rather have used continuous simulation techniques [41] to explore the time-behavior of the photochemical system. We are particularly interested in the effects of pulsed excitation, since the intensity-dependent experiments of both Burland *et al.* [36] and Dellinger *et al.* [37] were done using pulsed laser excitation.

The calculated response of a photochemical system obeying these kinetic equations is shown in Fig. 14. The parameters have been chosen to match the tetrazine example and to correspond to the experimental conditions of Fig. 10. These calculations assume a pulsed laser of 10 μJ and a pulse width of 5 ns. The extinction coefficient for step 1 (ϵ_1) is assumed to be 10^5 liter-mole^{-1}-cm^{-1}; for step 2 (ϵ_2), 10^2 liter-mole^{-1}-cm^{-1}. Other values were chosen to agree with the experimentally determined rates in s-tetrazine [32, 37]. After pulsed excitation, 60% of the molecules end up in excited states. The population of A_1^* (corresponding to the tetrazine S_1 state) approximately follows the laser pulse and quickly decays to the longer-lived intermediate state A_2^*. Of course, on time scales longer than those shown in the figure, the state A_2^* will eventually decay back to the ground state A.

If one looks at the concentration of the photoproduct A^{**} at the end of the laser pulse as a function of laser intensity I_0, one obtains the results shown in Fig. 15. Here we vary the total energy in the pulse, keeping the pulse width constant at 5 ns. The intensity is normalized to 1.0 for a 10-μJ, 5-ns pulse. At low laser light intensity the product concentration [A^{**}] depends quadratically on intensity. This is the intensity region over which the results

shown in Fig. 10(a) were obtained. At much higher laser intensities, not accessible in our experiments, the step $A \rightarrow A_1^*$ becomes very fast compared to other processes. The rate-determining step then becomes the absorption of the second photon. This leads to the linear dependence shown in Fig. 15. Recall that the second laser photon at 580 nm is inefficiently absorbed by the intermediate.

There is another possibility for linear intensity dependence. This occurs when the step $A_2^* \rightarrow A^{**}$ is fast compared to other steps in the process. Then the first photon absorption becomes rate-determining. This may explain the experimental results of Dellinger *et al.* [37]. With broad band lamp excitation, the first absorption step does not occur rapidly because of a relatively small total oscillator strength for the first transition. The second step $A_2^* \rightarrow A^{**}$ may, however, occur rapidly if the oscillator strength is high, because now the broad band lamp excitation has considerable overlap with the intermediate absorption (see Fig. 11).

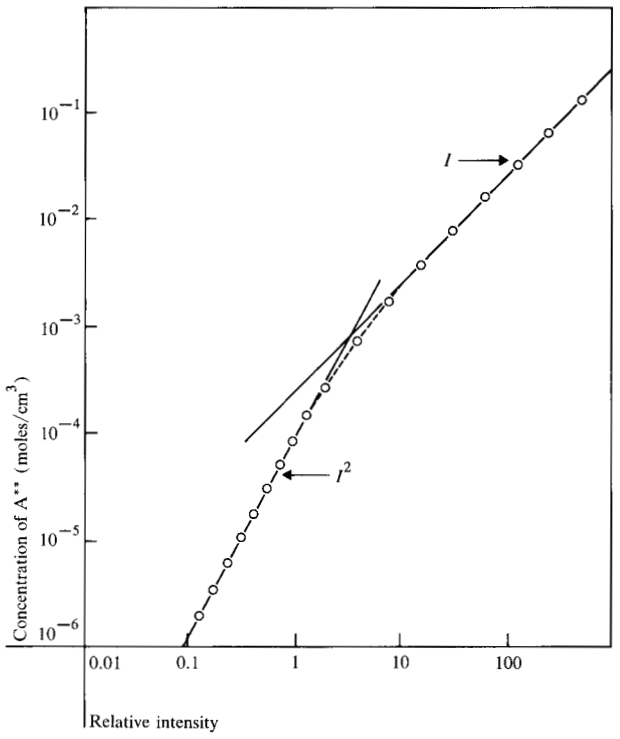

Figure 15 The concentration of the photoproduct A^{**} as a function of the laser light intensity (here 1.0 represents the intensity of a 10-μJ, 5-ns pulse). The lines represent the theoretical linear (I) and quadratic (I^2) responses.

Conclusions

We have described in detail the photochemical processes that can occur in solids at low temperatures. Of particular interest has been the development of a set of criteria that might lead to the utilization of this photochemistry in photochemical hole burning applications.

Because of the requirement that a PHB candidate exhibit a sharp zero-phonon line and the constraints this places on the system, it seems necessary that the state undergoing photochemistry and the state absorbing be different. We have presented two examples of PHB systems: quinizarin in hydrogen-bonded matrices and tetrazine in molecular crystals. The first of these examples undergoes a single-photon intermolecular proton exchange, and the second, a two-photon photodissociation.

Acknowledgments

The authors acknowledge the contributions of D. C. Alvarez, F. Carmona, F. Drissler, F. Graf, H.-K. Hong, A. Nazzal, and J. Pacansky to the work described in this paper. We also thank R. A. Caldwell and B. H. Schechtman for their valuable comments on the manuscript.

References and note

1. *Chemical and Biochemical Applications of Lasers*, Vol. 1, C. B. Moore, Ed., Academic Press, Inc., New York, 1974; S. Kimel and S. Speiser, *Chem. Rev.* **77,** 437 (1977); *Advances in Laser Chemistry*, A. H. Zewail, Ed., Springer-Verlag, Berlin, 1978.
2. G. Castro, D. Haarer, R. M. Macfarlane, and H. P. Trommsdorf, U.S. Patent 4,101,976, July 1978.
3. R. M. Hochstrasser and D. S. King, *J. Amer. Chem. Soc.* **97,** 4760 (1975); B. Dellinger, D. S. King, R. M. Hochstrasser, and A. B. Smith, *J. Amer. Chem. Soc.* **99,** 3197 (1977).
4. A. C. G. Mitchell and M. W. Zemansky, *Resonance Radiation and Excited States*, University Press, Cambridge, 1961; A. Schenzle and R. G. Brewer, *Phys. Rev. A* **14,** 1756 (1976).
5. S. Voelker, R. M. Macfarlane, H. P. Trommsdorff, and J. H. van der Waals, *J. Chem. Phys.* **67,** 1759 (1977); S. Voelker, R. M. Macfarlane, and J. H. van der Waals, *Chem. Phys. Lett.* **53,** 8 (1978).
6. T. J. Aartsma and D. A. Wiersma, *Chem. Phys. Lett.* **42,** 520 (1976); H. de Vries, P. de Bree, and D. A. Wiersma, *Chem. Phys. Lett.* **52,** 399 (1977); A. H. Zewail, D. E. Godar, K. E. Jones, T. E. Orlowski, R. R. Shah, and A. Nichols, *Proc. Soc. Photo-optical Instrumen. Engineers (SPIE)* **113,** 42 (1977); R. M. Macfarlane, A. Z. Genack, and R. G. Brewer, *Phys. Rev. B* **17,** 2821 (1978).
7. D. B. Fitchen, R. S. Silsbee, T. A. Fulton, and E. L. Wolf, *Phys. Rev. Lett.* **11,** 215 (1963).
8. G. F. Imbusch, W. M. Yen, A. L. Schawlow, D. E. McCumber, and M. D. Sturge, *Phys. Rev. A* **133,** 1029 (1964).
9. N. Bloembergen, E. M. Purcell, and R. V. Pound, *Phys. Rev.* **73,** 679 (1948).
10. C. P. Slichter, *Principles of Magnetic Resonance*, Harper and Row, New York, 1963.
11. A. Szabo, *Phys. Rev. B* **11,** 4512 (1975).
12. B. M. Kharlamov, R. I. Personov, and L. A. Dykovskaya, *Opt. Commun.* **12,** 191 (1974).
13. A. A. Gorokhovskii, R. K. Kaarli, and L. A Rebane, *JETP Lett.* **20,** 216 (1974).
14. A. A. Gorokhovskii, R. K. Kaarli, and L. A. Rebane, *Opt. Commun.* **16,** 282 (1976).
15. H. de Vries and D. A. Wiersma, *Phys. Rev. Lett.* **36,** 91 (1976).

16. D. Haarer, *J. Chem. Phys.* **67,** 4076 (1977).
17. D. M. Burland, *Chem. Phys. Lett.* **36,** 247 (1975).
18. J. M. Hayes and G. J. Small, *Chem. Phys.* **27,** 151 (1978).
19. S. Voelker and J. H. van der Waals, *Mol. Phys.* **32,** 1703 (1976).
20. F. Graf, H.-K. Hong, A. Nazzal, and D. Haarer, *Chem. Phys. Lett.* **59,** 217 (1978).
21. J. A. Pople and D. L. Beveridge, *Approximate Molecular Orbital Theory*, McGraw-Hill Book Co., Inc., New York, 1970, p. 111.
22. D. Hall and C. L. Nobbs, *Acta Cryst.* **21,** 927 (1966).
23. E. V. Shpol'skii, *Sov. Phys. Usp.* **3,** 372 (1960); **5,** 522 (1962); **6,** 411 (1963).
24. F. Drissler, F. Graf, and D. Haarer, unpublished results.
25. W. Klopfer, in *Advances in Photochemistry*, Vol. 10, W. A. Noyes, Jr., G. S. Hammond, and J. N. Pitts, Jr., Eds., Wiley-Interscience, New York, 1977, p. 311ff.
26. G. J. Brealey and M. Kasha, *J. Amer. Chem. Soc.* **77,** 4462 (1955).
27. J. J. Markham, *Rev. Mod. Phys.* **31,** 956 (1959).
28. M. N. Sapozhnikov, *Phys. Stat. Solidi B* **75,** 11 (1976).
29. G. E. Busch, M. L. Applebury, A. A. Lamola, and P. M. Rentzepis, *Proc. Nat. Acad. Sci.* **69,** 2802 (1972); K. Peters, M. L. Applebury, and P. M. Rentzepis, *Proc. Nat. Acad. Sci.* **74,** 3119 (1977).
30. A. Muller and E. Pfluger, *Chem. Phys. Lett.* **2,** 155 (1968); H. S. Pilloff and A. C. Albrecht, *J. Chem. Phys.* **49,** 4891 (1968); K. Razi Naqvi, D. K. Sharma, and G. J. Hoytink, *Chem. Phys. Lett.* **22,** 222, 226 (1973); J. Kolc and J. Michl, *J. Amer. Chem. Soc.* **92,** 4147, 4148 (1970).
31. V. F. Mandzhikov, A. P. Darmanyan, V. A. Barachevskii, and Y. N. Gerulaitis, *Opt. Spekt.* **32,** 412 (1972).
32. R. M. Hochstrasser, D. S. King, and A. C. Nelson, *Chem. Phys. Lett.* **42,** 8 (1976); R. M. Hochstrasser and D. S. King, *J. Amer. Chem. Soc.* **98,** 5443 (1976); R. M. Hochstrasser, D. S. King, and A. B. Smith, *J. Amer. Chem. Soc.* **99,** 3923 (1977).
33. H. de Vries and D. A. Wiersma, *Chem. Phys. Lett.* **51,** 565 (1977).
34. R. R. Karl and K. K. Innes, *Chem. Phys. Lett.* **36,** 275 (1975).
35. J. H. Meyling, R. P. van der Werf, and D. A. Wiersma, *Chem. Phys. Lett.* **28,** 364 (1974).
36. D. M. Burland, *Proc. SPIE* **113,** 151 (1977); D. M. Burland, F. Carmona, and J. Pacansky, *Chem. Phys. Lett.* **56,** 221 (1978).
37. B. Dellinger, M. A. Paczkowski, R. M. Hochstrasser, and A. B. Smith, *J. Amer. Chem. Soc.* **100,** 3242 (1978).
38. D. M. Burland and F. Carmona, *Mol. Cryst. Liq. Cryst.*, in press.
39. E. L. Simmons, *J. Phys. Chem.* **75,** 588 (1971); E. L. Simmons and W. W. Wendlandt, *Coord. Chem. Rev.* **7,** 11 (1971).
40. H. Mauser, *Z. Naturforsch.* **22b,** 569 (1967).
41. The high-level language that we used is known as DSL/dp; it was developed by M. H. Dost, W. M. Syn, N. N. Turner, and D. G. Wyman.

Received March 5, 1979; revised March 27, 1979

The authors are located at the IBM Research Division laboratory, 5600 Cottle Road, San Jose, California 95193.